J Neurophysiol
87: 2808–2816, 2002; 10.1152/jn.00590.2001.

Voluntary Control of Static Endpoint Stiffness During Force Regulation Tasks

ERIC J. PERREAULT,[1–3] ROBERT F. KIRSCH,[2,3] AND PATRICK E. CRAGO[2,3]
[1]*Northwestern University Medical School, Chicago, Illinois 60611; and* [2]*Case Western Reserve University and* [3]*Louis Stokes Veterans Affairs Medical Center, Cleveland, Ohio 44106*

Received 18 July 2001; accepted in final form 24 January 2002

Perreault, Eric J., Robert F. Kirsch, and Patrick E. Crago. Voluntary control of static endpoint stiffness during force regulation tasks. *J Neurophysiol* 87: 2808–2816, 2002; 10.1152/jn.00590.2001. The goals of this study were to determine the degree to which subjects could voluntarily modulate static endpoint stiffness orientation and to quantify the effects of simultaneously generated voluntary endpoint forces on this ability. Static endpoint stiffness, which characterizes the relationship between externally imposed displacements of the hand and the elastic forces generated in response, was estimated in real time during the application of planar, stochastic perturbations of endpoint position. This estimation was accomplished using a real-time parametric identification algorithm on measured force and position data. Subjects were provided with real-time visual feedback of endpoint stiffness, and their ability to modulate the orientation of maximum static stiffness was measured for different endpoint force magnitudes and directions. We found that individuals *can* voluntarily change stiffness orientation but that the magnitude of these changes is small, the range of available stiffness orientations decreases as endpoint force exertion increases, and endpoint force direction significantly constrains direction and magnitude of the stiffness orientations that can be achieved. Given these findings it appears unlikely that static endpoint stiffness orientation is controlled independently of force by voluntary neural mechanisms during postural tasks.

INTRODUCTION

The human arm presents a stable mechanical interface to its environment, allowing it to make reliable contact with a variety of objects and to maintain stable postures in the face of uncertain and often destabilizing loads. Understanding how the mechanical properties of the arm, specifically its endpoint stiffness, are modified during functional tasks may elucidate the underlying neuromotor control strategies. The goal of this study was to determine whether the orientation of maximum static endpoint stiffness could be controlled voluntarily during postural tasks. Our results indicate that, during the maintenance of posture, control over endpoint stiffness orientation is limited and appears to be largely constrained by tasks that involve exerting forces on the environment.

Endpoint stiffness, defined as the relationship between externally applied displacements of the hand and the forces generated in response, was used to characterize arm mechanics. It is thought that such stiffness measurements are related closely to postural stability (Bizzi and Abend 1983; Colgate and Hogan 1988; Feldman 1966; Gomi and Osu 1998; Hogan 1985; Lacquaniti et al. 1993). Hogan (1985) first proposed that arm stability might be maintained via regulation of endpoint-stiffness properties. Since then, several studies have examined how the multi-joint-stiffness properties of the human arm are modulated during different tasks (Dolan et al. 1993; Gomi and Kawato 1997; Mussa-Ivaldi et al. 1985; Tsuji et al. 1995), but few have examined the degree to which these properties can be controlled voluntarily. It is well known that increased cocontraction of agonist and antagonist muscles increases stiffness both at the single- and multi-joint levels (see Kearney and Hunter 1990 for a review). This represents one aspect of endpoint stiffness that is under voluntary control, but it is unclear whether finer control over the endpoint stiffness characteristics exists. Endpoint stiffness properties are directional, providing greater resistance to externally applied perturbations in certain directions than others (Dolan et al. 1993; Gomi and Osu 1998; Mussa-Ivaldi et al. 1985; Perreault et al. 2001; Tsuji et al. 1995). The ability to control maximum and minimum stiffness orientation could allow significant flexibility during tasks with direction-dependent constraints such as ball-catching, where increased stiffness is only required along the line of impact of the ball with the hand, or during tool manipulation, where kinematic environmental constraints may require a compliant interface in one direction but stability constraints may require high stiffness in another direction. Few studies have investigated the ability to modulate endpoint stiffness orientation. Lacquaniti et al. (1993) showed that the orientation of endpoint viscous properties rotates toward the direction of impact when preparing to catch a ball, and Gomi and Osu (1998) showed that static endpoint stiffness orientation could be manipulated with changes in muscle cocontraction. Recent work by Burdet et al. (2001) also demonstrated that static stiffness orientation is modified to compensate for environmental instabilities during movement. These studies provided evidence that the directional properties of endpoint stiffness can be modulated. However, none of these studies addressed the extent of stiffness modulation, nor how this modulation is affected by voluntarily generated endpoint forces. Furthermore, the movement and ball-catching tasks were largely subconscious because no stiffness/viscous feedback was provided

Address for reprint requests: E. J. Perreault, Dept. of Physiology, Ward 5-295, Northwestern University Medical School, 303 E. Chicago Ave., Chicago, IL 60611 (E-mail: e-perreault@northwestern.edu).

The costs of publication of this article were defrayed in part by the payment of page charges. The article must therefore be hereby marked ''*advertisement*'' in accordance with 18 U.S.C. Section 1734 solely to indicate this fact.

and were concerned with transient rather than sustained changes in stiffness orientation.

This study had two specific goals. The first was to determine the degree to which subjects could maintain voluntarily changes in static endpoint stiffness orientation. The second was to quantify the effects of voluntarily generated endpoint forces on this ability. To accomplish these goals, we provided subjects with real-time visual feedback of endpoint stiffness and gave them specific suggestions on how to modify this stiffness. We found that individuals *can* voluntarily change stiffness orientation but the magnitude of these changes is small, the range of voluntarily modifiable stiffness orientations decreases as endpoint force exertion increases, and endpoint force direction determines direction and magnitude of the stiffness orientations that can be achieved. Portions of this work have been presented previously in abstract form (Perreault et al. 2000).

METHODS

Apparatus

Endpoint stiffness was estimated using perturbations applied by a two-joint robotic manipulator described in detail previously (Acosta et al. 2000) and summarized briefly in the following text. Figure 1*A* illustrates this device, which was configured as a position servo for these experiments. Subjects were strapped into a rigid chair with custom supports to constrain both lateral and anterior-posterior trunk movements. Each subject's arm was attached to the manipulator endpoint via a custom-fitted fiberglass cast that was free to pivot in the horizontal plane about the attachment point. Each subject's cast rigidly fixed the wrist joint and covered approximately three-quarters of the forearm. The manipulator was instrumented to measure the displacements of the subject's hand and the forces applied between the subject and the manipulator.

Perturbation characteristics

During each experiment, the manipulator applied a bandlimited stochastic position perturbation to the subject's hand. The x and y components of this perturbation were nearly independent and had peak-to-peak amplitudes of approximately 2 cm. The resulting endpoint force amplitude varied from trial to trial depending on the arm stiffness. Figure 2*A* shows typical endpoint displacement and force recordings. The displacement frequency content was designed to be within the range of physiologically encountered perturbations (Mann et al. 1989) yet to contain enough information for adequate identification of the endpoint dynamics. Figure 2*B* shows the spectra of the endpoint perturbations used in this study. The perturbation spectrum was flat to 3 Hz, above which it declined at a rate of 40 dB/decade.

To improve the real-time estimation of the static components of endpoint stiffness (see next section), the higher frequency components of displacement and force were removed by low-pass filtering at 5 Hz with 8-pole elliptical filters (Iotech, Cleveland OH; Filter488/8 FL2). Signals were then sampled at 100 Hz with a 12-bit data-acquisition board (National Instruments, Austin, TX; AT-MIO-16).

Endpoint stiffness estimation

Endpoint stiffness describes the dynamic relationship between displacements imposed at the hand (x, y) and the forces effecting those displacements (f_x, f_y). In these experiments, stiffness was estimated while subjects maintained a constant arm posture in the horizontal plane. Previous studies (Dolan et al. 1993; Perreault et al. 1999; Stroeve 1999; Tsuji et al. 1995) have shown that under these postural conditions, a model with inertial (I_{end}), viscous (B_{end}), and elastic (K_{end}) terms can characterize the endpoint stiffness dynamics. For measurements in the horizontal plane, this mathematical model has the form given by *Eq. 1*

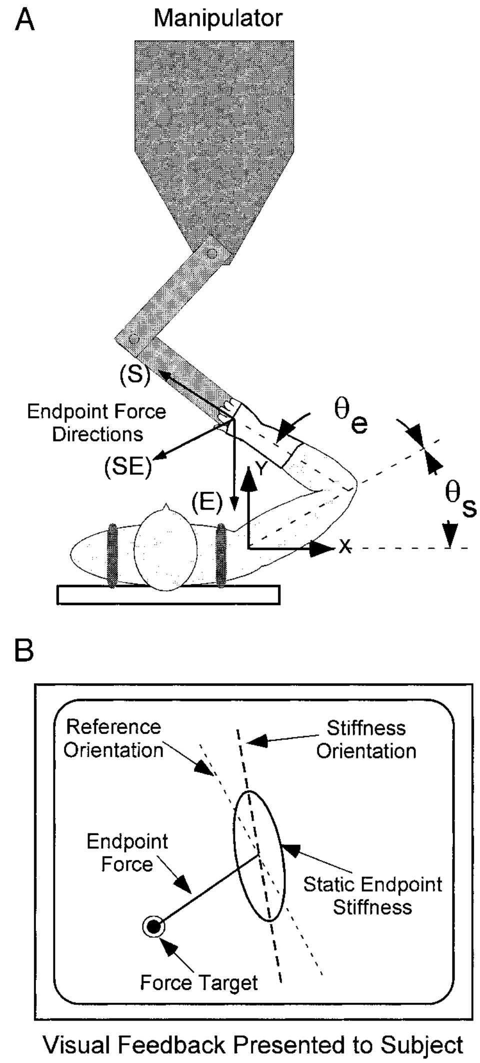

FIG. 1. Experimental setup. *A*: a 2-joint robotic manipulator was used to apply endpoint perturbations in these experiments. During each trial, subjects exerted a constant force on the manipulator in 1 of the 3 directions shown at either 10 or 20% maximum voluntary contraction (MVC). Direction S required only shoulder torques, direction E only elbow torques, and direction SE both shoulder and elbow torques. *B*: the visual feedback provided to the subject. Feedback includes a current estimate of static endpoint stiffness, an endpoint force target, and a reference orientation as measured during the N task, where subjects matched the endpoint force target without regard for stiffness orientation.

$$[I_{\text{end}}]\begin{bmatrix} \ddot{x} \\ \ddot{y} \end{bmatrix} + [B_{\text{end}}]\begin{bmatrix} \dot{x} \\ \dot{y} \end{bmatrix} + [K_{\text{end}}]\begin{bmatrix} x \\ y \end{bmatrix} = \begin{bmatrix} f_x \\ f_y \end{bmatrix}; \quad \text{where}$$

$$[I_{\text{end}}] = \begin{bmatrix} I_{xx} & I_{xy} \\ I_{yx} & I_{yy} \end{bmatrix}, \quad [B_{\text{end}}] = \begin{bmatrix} B_{xx} & B_{xy} \\ B_{yx} & B_{yy} \end{bmatrix}, \quad [K_{\text{end}}] = \begin{bmatrix} K_{xx} & K_{xy} \\ K_{yx} & K_{yy} \end{bmatrix} \quad (1)$$

The elastic properties of the arm are directionally dependent, meaning that the static resistance to external perturbations of hand posture depends on the orientation of the perturbation. This dependence on direction can be represented graphically by transforming the static endpoint stiffness matrix into an ellipse, as was first demonstrated by Mussa-Ivaldi (Mussa-Ivaldi et al. 1985). *Equation 2* demonstrates this mapping. The variables $F_y^K(t)$ and $F_x^K(t)$ represent the elastic components of the force response for unit displacements of the hand in endpoint position along all directions in the plane; these unit displace-

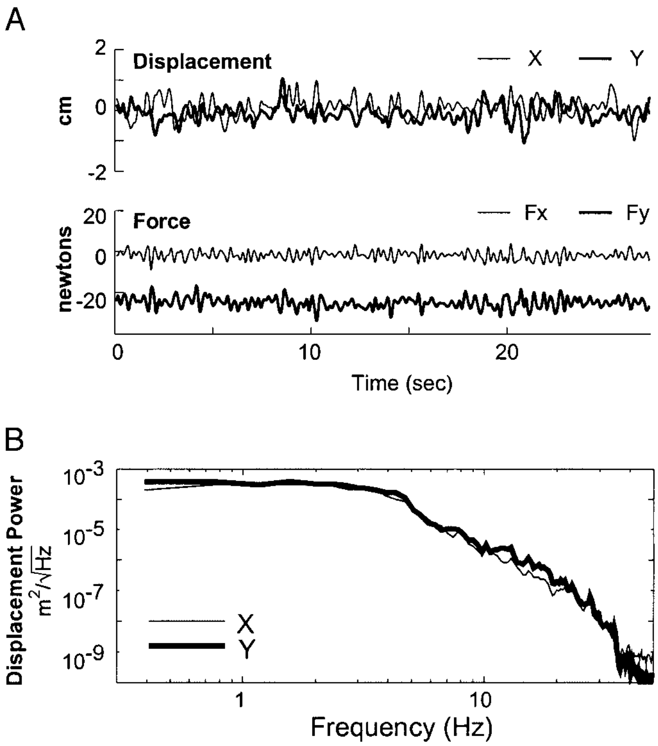

FIG. 2. Typical data. *A*: typical endpoint displacements and forces. *B*: the power spectrum of the applied position perturbations.

ments are generated using the sin and cos functions in *Eq. 2*. The ellipse representing the directional properties of K_{end} is generated by plotting $F_y^K(t)$ against $F_x^K(t)$

$$\begin{bmatrix} F_x^K(t) \\ F_y^K(t) \end{bmatrix} = K_{\text{end}} \cdot \begin{bmatrix} \cos(t) \\ \sin(t) \end{bmatrix}; \quad \text{where} \quad 0 < t < 2\pi \tag{2}$$

The major axis of the ellipse denotes the direction along which the hand is most resistant to static perturbations of posture and the minor axis the direction along which the hand is least resistant to these perturbations. These ellipses can be characterized by the orientation of the major axis, ϕ, the shape or ratio of the minor to major axis lengths, *s*, and the area, *A*. The equations needed to calculate each of these parameters were presented by Gomi and Osu (1998) and are repeated in the following text for completeness. Note that they do not require the parameter matrix to be symmetric. $\lambda(.)$ represents the eigenvalue operator.

$$\phi = \tan^{-1}\left(\frac{U_{\max\_y}}{U_{\max\_x}}\right) \tag{3}$$

where $U_{\max\_x}$ and $U_{\max\_y}$ are obtained via singular value decomposition of the K_{end} matrix (Golub and Van Loan 1996)

$$K_{\text{end}} = U \cdot S \cdot V^T, \quad \text{and} \quad U = \begin{bmatrix} U_{\max\_x} & U_{\min\_x} \\ U_{\max\_y} & U_{\min\_y} \end{bmatrix} \tag{4}$$

$$\text{shape} = \frac{\alpha_{\min}}{\alpha_{\max}}, \quad \text{where} \quad \alpha_{\min} = \sqrt{\lambda_{\min}(K_{\text{end}}^T \cdot K_{\text{end}})} \quad \text{and}$$

$$\alpha_{\max} = \sqrt{\lambda_{\max}(K_{\text{end}}^T \cdot K_{\text{end}})} \tag{5}$$

$$\text{Area} = \pi \alpha_{\min} \alpha_{\max} \tag{6}$$

A multiple-input multiple-output recursive least-squares system identification algorithm (Ljung 1987) was implemented to provide real-time estimates of endpoint stiffness by estimating the parameters of *Eq. 1* from the recorded endpoint forces and displacements. Similar algorithms have been used to estimate time-varying stiffness during movement (Bennett et al. 1992; Gomi and Konno 1998). Because a multiple-input multiple-output algorithm was used, the minimal coupling between the applied *x* and *y* position perturbations did not bias the estimated stiffness parameters (Perreault et al. 1999). To improve estimation accuracy, the inertia matrix was estimated while the subject was at rest and instructed not to react to the applied perturbation. The inertia matrix estimated under these conditions was fixed for the remainder of the trials. The use of a real-time estimation algorithm allowed subjects to view specific characteristics of endpoint stiffness during each experimental trial. Parameter estimates were updated at each sample instant (10 ms) and made available for real-time feedback to the subject every 500 ms. Figure 3 illustrates how this algorithm tracks changes in static stiffness orientation using simulated data. These simulations involved applying random endpoint displacements to a dynamic model of the arm (*Eq. 1*) with known inertial, viscous, and elastic parameters. Random noise with a spectral content and signal-to-noise ratio matching the actual experimental data were added to the simulated endpoint forces. At the time indicated by 0 s on the graph, the simulated static arm stiffness was increased and rotated counter clockwise, as illustrated by the ellipses at the *top* of Fig. 3. The horizontal bars indicate the actual orientation of the simulated static endpoint stiffness. The black trace shows the progression of the real-time estimate of orientation. It is seen that the orientation estimate reaches the true value approximately 15 s after the change in endpoint stiffness dynamics. This represents typical performance of the real-time estimation algorithm. The long time required for adaptation in these experiments is due to the low-pass nature of the arm dynamics, which can have a cutoff frequency as low as 1 Hz during resting conditions (Perreault 2000). The speed of adaptation can be increased, but at the cost of increasing the noise of the estimate, thereby degrading visual feedback quality. We were interested in the ability to modify and maintain endpoint stiffness properties, so we opted for the slower but more accurate estimation parameters.

The endpoint stiffness of the arm is directly dependent on the stiffness of the elbow and shoulder joints and the coupling stiffnesses acting between these joints. To provide insight to the physiological mechanisms regulating endpoint stiffness mechanics, joint-stiffness parameters were computed off-line using the endpoint parameters estimated during each experiment and *Eq. 7* (McIntyre et al. 1996). In this equation, *J* is the Jacobian relating differential changes in joint rotation to differential changes in endpoint displacement, l_{h} and l_{f} are

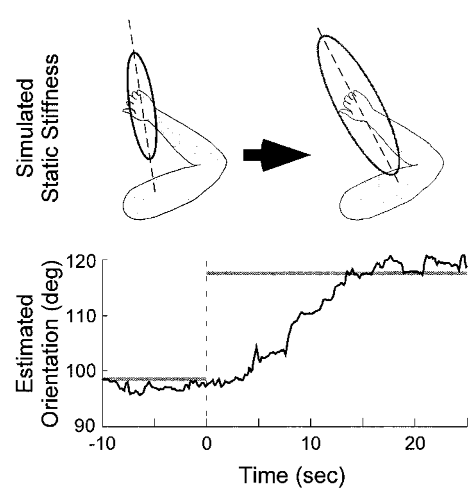

FIG. 3. Real-time parameter estimation. Simulated tracking of endpoint stiffness orientation. Ellipses indicate initial and final simulated static endpoint stiffness, which was changed at $t = 0$ s. The horizontal bars indicate the actual orientation of the simulated static endpoint stiffness, and the black trace shows the progression of the real-time estimate.

the lengths of the humerus and forearm, θ_s and θ_e are the shoulder and elbow angles, and F_{end} is the steady-state endpoint force vector. K_{ss} is the stiffness of the shoulder joint, K_{ee} is the stiffness of the elbow joint, and K_{es} and K_{se} are the stiffnesses acting between these joints (see Hogan 1985)

$$K_{jnt} = \begin{bmatrix} K_{ss} & K_{se} \\ K_{es} & K_{ee} \end{bmatrix} = J^T \cdot K_{end} \cdot J + \frac{\partial J^T}{\partial \Theta} F_{end}$$

$$J = \begin{bmatrix} -l_h \sin(\theta_s) - l_f \sin(\theta_s + \theta_e) & -l_f \sin(\theta_s + \theta_e) \\ l_h \cos(\theta_s) + l_f \cos(\theta_s + \theta_e) & l_f \cos(\theta_s + \theta_e) \end{bmatrix} \quad (7)$$

The joint-stiffness matrix can be decomposed into symmetric and anti-symmetric components, as shown in *Eq. 8* (Hogan 1985). All joint-stiffness matrices estimated in this study were predominantly symmetric. Therefore to facilitate analyzing the coupling between joints, only the symmetric component of the joint-stiffness matrix was used in subsequent analyses. The cross term of the symmetric joint-stiffness matrix, K_x, is the average of the cross terms, K_{es} and K_{se}, in the original joint-stiffness matrix. It represents the joint stiffness contributed by muscles crossing the elbow and shoulder joints. The stiffness of these two-joint muscles couples actions at the shoulder and elbow and also contributes to the estimated stiffness of these individual joints. The stiffness of the elbow and shoulder joints, K_{ee} and K_{ss} in *Eq. 7,* represent the sum of the stiffness contributed by the single joint muscles crossing each joint, K_e and K_s, and the stiffness contributed by the muscles crossing both joints, as represented in *Eq. 8.*

$$K_{jnt} = K_{j\_a} + K_{j\_s}$$

$$K_{j\_a} = \frac{K_{jnt} - K_{jnt}^T}{2}$$

$$K_{j\_s} = \frac{K_{jnt} + K_{jnt}^T}{2} = \begin{bmatrix} K_s + K_x & K_x \\ K_x & K_e + K_x \end{bmatrix} \quad (8)$$

Subjects and protocol

Four healthy subjects ranging from 23 to 40 yr and with no history of neurological impairments were used in this study. Subjects gave informed consent to all procedures and were free to withdraw from the study at any time. All measurements were made on the right arm, which happened to be the dominant arm of each subject. Subjects were not naïve with respect to the experimental protocol. Each had been involved previously in similar endpoint perturbation studies and was also familiar with the concept of static endpoint stiffness. Hence, each was able to understand the concepts and instructions in the protocol outlined in the following text.

A single arm posture was used in these experiments. The arm of each subject was positioned in the horizontal plane passing through the glenohumeral joint with the endpoint located in front of this joint at a distance of approximately 0.3 m forward of the acromion. Table 1 gives the measured elbow (θ_e) and shoulder joint (θ_s) angles in degrees and hand locations (*x, y*) in meters relative to the acromion for each subject.

During these experiments, subjects were required to exert constant forces against the manipulator. The magnitude of these forces was scaled relative to each subject's maximum voluntary contraction (MVC) as determined in a previous set of experiments (Perreault et al. 2001) in which subjects were required to exert MVCs along the $\pm x$ and $\pm y$ axes illustrated in Fig. 1*A*. These MVCs were recorded at three endpoint locations, the one used in this study and two others at the same anterior distance from the shoulder. One of these was located in front of the sternum and the other approximately 0.2 m lateral to the acromion. The minimum of these 12 MVCs represents a general measure of arm strength and was used to scale the voluntary effort in these experiments. This endpoint force will be referred to as the MVC for each subject. Table 1 reports the values for each subject.

Subjects were instructed to exert forces against the manipulator with magnitudes of 0, 10, or 20% of their MVC. Three different force directions were used as indicated in Fig. 1*A*. Force direction S was directed along the line from the elbow to the hand and required only torques about the shoulder joint; force direction E was directed from the hand to the shoulder and required only torques about the elbow joint. Force direction SE was halfway between S and E and required torques about both the elbow and shoulder joints. A continuous visual display of endpoint force as well as a real-time estimate of static endpoint stiffness was provided to the subjects as illustrated in Fig. 1*B*. Both the static endpoint stiffness ellipse and its major axis were displayed. For each endpoint force, subjects were given one of three possible tasks: to reach the specified force target in the most natural manner without regard to endpoint stiffness (N task), to rotate the static endpoint stiffness ellipse as far as possible clockwise (CW task) relative to the N task, and to rotate the static endpoint stiffness ellipse as far as possible counter-clockwise (CCW task) relative to the N task. The orientation recorded for the N task was displayed as a reference during both the CW and CCW tasks. Based on the results of Gomi and Osu (1998), subjects were told that increased cocontraction of the elbow muscles tended to generate CW rotations of endpoint stiffness orientation and that increased cocontraction of the shoulder muscles tended to generate CCW rotations. Subjects, though, were not limited to these strategies.

Each combination of task, force magnitude, and force direction was tested once per session, resulting in a total of 21 experimental trials per session (3 tasks $\times$ 2 magnitudes $\times$ 3 directions $=$ 18 nonzero force trials, plus 3 tasks at 0 endpoint force $=$ 21 trials). To observe learning-related effects on performance, six sessions were recorded for each subject on six separate days. During each session, all trials were performed separately with a minimum rest period of 1 min between trials. All tasks for a given force magnitude and direction were performed sequentially; the N task was always performed first to provide the reference stiffness orientation, but the order of the CW and CCW tasks were randomized. The target force magnitude and direction used in each block of three tasks were also selected randomly, and a subsequent regression analysis on the times required to complete each trial indicated that trial order did not influence task performance.

In each trial, static endpoint stiffness was recorded only after the orientation had remained stable for more than 10 s to compensate for the delays in the real-time estimation algorithm. Because the algorithm took approximately 15 s to converge to a stable estimate (Fig. 3), the 10-s requirement before data collection meant that subjects had to maintain a constant level of effort for 25 s. In addition to the stiffness orientation requirements, trials were only considered to be successful if subjects matched the endpoint force target to within 1% of the previously measured MVC throughout the entire 25-s period. Due to these strict requirements, subjects found it difficult to modulate endpoint stiffness orientation while simultaneously matching a target endpoint force. This difficulty was evident in the increased time required to complete the CW and CCW tasks relative to that required for the N task (33.2 s, $P = 0.03$) as measured during the final data set collection for each subject. Because of this reported difficulty, subjects were allowed to rest following unsuccessful attempts to complete a task. No strict limits were set on the time allowed for task comple-

TABLE 1. *Subject-dependent experimental parameters*

Subject	θ_s	θ_e	x	y	MVC, N
1	41.7	103.3	−0.02	0.40	200
2	21.4	120.6	0.01	0.28	80
3	19.5	117.9	0.03	0.32	180
4	23.3	124.6	0.01	0.29	150

MVC, maximum voluntary contraction.

tion, although by the final session, 90% of trials were completed in less than 2 min, including any self-imposed rest periods.

Statistics

The experimental data set consisted of a single outcome measure per trial, endpoint stiffness orientation, and three independent factors: force magnitude, force direction, and the task given to the subject (N, CW, or CCW). The goal of this analysis was to quantify subjects' ability to modulate static endpoint stiffness orientation and to determine how voluntarily generated endpoint forces affected this ability. Three variables related to orientation were computed for each endpoint force condition: the total range over which stiffness orientation could be modulated, the portion of this range due to clockwise rotations relative to the orientation during the N task, and the portion due to counter-clockwise rotations relative to the orientation during the N task. The equations used for these computations are summarized in the following text.

$$\text{Range} = \phi_{\text{CCW}} - \phi_{\text{CW}} = \Delta\phi_{\text{CW}} + \Delta\phi_{\text{CCW}}$$

$$\Delta\phi_{\text{CW}} = \phi_{\text{N}} - \phi_{\text{CW}}$$

$$\Delta\phi_{\text{CCW}} = \phi_{\text{CCW}} - \phi_{\text{N}} \quad (9)$$

where ϕ_{CCW} is the ellipse orientation when the subject was performing the CCW task, ϕ_{CW} is the ellipse orientation when the subject was performing the CW task, and ϕ_{N} is the orientation when the subject was performing the N task. The influences of force magnitude and force direction on the three measures of stiffness modulation listed in *Eq. 9* were assessed using a repeated-measures ANOVA (Montgomery 1991). Because force direction is not defined for the 0% MVC trials, this data could not be incorporated into the ANOVA analysis. Statistics from the 0% MVC trials simply represent the trial means with errors adjusted for inter-subject variability as is done for the repeated-measures ANOVA. All statistical calculations were performed using S-Plus (MathSoft, Cambridge, MA).

RESULTS

Algorithm performance

The real-time identification algorithm used in this study gave accurate estimates of static endpoint stiffness. The accuracy and bias of the real-time algorithm was compared with the nonparametric off-line approach we have used previously that is a robust estimator of endpoint stiffness dynamics (Perreault et al. 1999, 2001). To compare these methods, 17 data sets for each subject were analyzed using both algorithms. The data set for each subject was similar to the data collected in this experiment during the N task. The 17 trials corresponded to four different force magnitudes equally spaced from 7.5 to 30% MVC and four different force directions oriented along the $\pm x$ and the $\pm y$ axes indicated in Fig. 1; the final trial was recorded with no endpoint force exertion. The difference in static stiffness orientation computed by the two algorithms was $0.91 \pm 5.85°$ (mean $\pm$ SD) across all 68 data sets. The stiffness magnitude in all directions also was estimated consistently by both algorithms as quantified by the shape and area differences which were 3 ± 6 and $12 \pm 15\%$, respectively. These results indicate that the real-time estimates of orientation were virtually identical to those obtained by the well-characterized off-line techniques. All subsequent results were estimated by the real-time algorithm.

Learning effects

Subjects' abilities to modulate the range of endpoint stiffness orientations increased over the six experimental sessions ($P = 0.037$), indicating a learning effect. This effect was significant in the first three sessions but was not present after the third session ($P = 0.48$). Even across the first three sessions, the average increase in range was only 2.8°. To completely eliminate these learning effects, however, only data from the final three sessions were used for the remainder of this analysis.

Endpoint stiffness modulation

Figure 4 shows an example of one subject's ability to modulate static endpoint stiffness orientation. Note that this subject modulated endpoint stiffness orientation more readily than any other subject. The figure illustrates the estimated static endpoint stiffness for the 10% MVC force in the three tested directions. The center of each ellipse is positioned along the direction that the subject was exerting force against the manipulator as indicated by the black arrows. There are three ellipses at each location, corresponding to the three tasks the subjects were asked to perform at each force level. The black ellipses indicate the estimated static stiffness when the subject was exerting force naturally, i.e., without regard to stiffness orientation (condition N). The light gray ellipses correspond to the CW task and the dark gray ellipses to the CCW task. When the subject was exerting forces that required only torques about the shoulder (S), the endpoint stiffness could be rotated over a

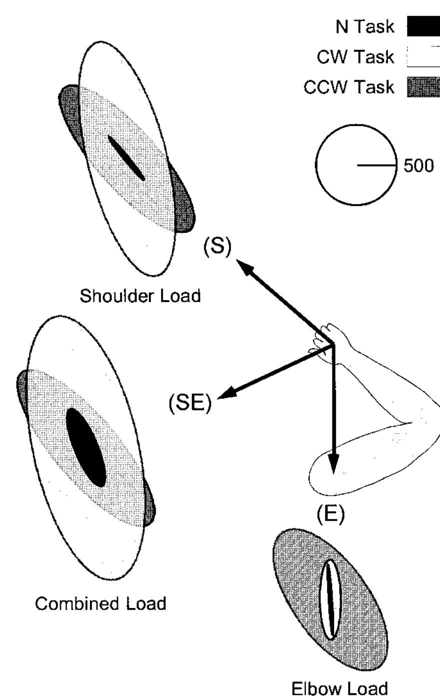

FIG. 4. Endpoint stiffness rotation. Shows 1 subject's (*4*) ability to modulate static endpoint stiffness orientation for 10% MVC loads in the 3 tested directions. The center of each ellipse is positioned along the direction that the subject was exerting force against the manipulator as indicated by the black arrows. The 3 ellipses at each location correspond to the 3 tasks the subjects were asked to perform at each force level. The black ellipses indicate "natural" force exertion (N), the light gray ellipses correspond to the clockwise (CW) task and the dark gray ellipses to the counter-clockwise (CCW) task.

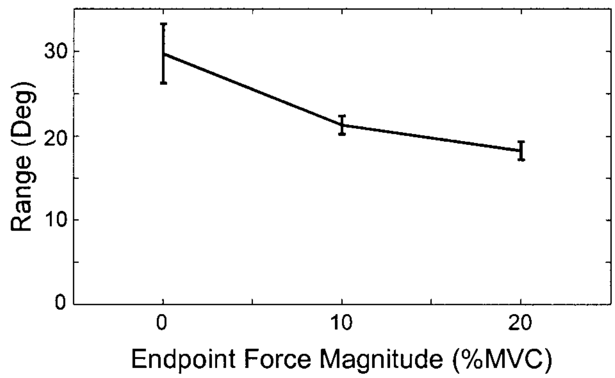

FIG. 5. Effects of force magnitude. The average effect of force magnitude on the range of obtainable endpoint stiffness orientations for all subjects is shown. Error bars indicate ±SE as estimated from a repeated-measures ANOVA.

modest range in the clockwise direction, but only very little in the counter-clockwise direction. The opposite effect was seen when the subject matched endpoint forces requiring only elbow torques (E)—the subject could produce modest stiffness orientation rotation in the counter-clockwise direction but little or no rotation in the clock-wise direction. Both clockwise and counter-clockwise rotations could be achieved when exerting the endpoint force that required both elbow and shoulder torques (SE).

STRATEGIES FOR MODULATING STIFFNESS ORIENTATION. Figure 4 also illustrates that stiffness ellipse area (i.e., magnitude) increased during attempts to voluntarily modulate stiffness orientation, indicating the use of cocontraction. Increased cocontraction was most evident during tasks when subjects successfully rotated stiffness orientation away from the natural direction. Subjects adopted one of two different strategies, though, when significant orientation changes could not be achieved readily. Figure 4 shows an example of both strategies. The first involved minimal increases in muscle cocontraction. For example, when this subject was exerting an endpoint force that required only elbow torques (E), he was not able to generate large clockwise rotations relative to the natural direction. In this case, he used only a small degree of cocontraction, as evidenced by the small increase in ellipse size. The second strategy involved large increases in cocontraction, even though the resulting stiffness rotation remained small. This strategy was employed when the subject attempted to generate counter clockwise rotations while exerting an endpoint force that required only shoulder torques (S). The median stiffness area for all subjects increased by 383% for the CW and CCW tasks relative to the N task. This increase was greatest for trials where the stiffness orientation could be rotated by more than 5° relative to the N task (553%). Trials in which stiffness orientation could be rotated by less than 5° had a median area that was 227% larger than that of the corresponding N tasks. These results suggest that cocontraction was used to a greater extent in the in the trials where stiffness orientation could be successfully modulated.

EFFECTS OF FORCE MAGNITUDE. The ability to modulate endpoint stiffness orientation decreased with increasing endpoint force. The range of stiffness orientation modulation depended only on endpoint force magnitude ($P = 0.051$) and not on force direction ($P = 0.36$). Figure 5 shows how this range (±SE) varied with endpoint force for all subjects. There was an average decrease in modulation range from 29.8 to 18.3° as the endpoint force increased from 0 to 20% MVC.

EFFECTS OF FORCE DIRECTION. The orientation of the endpoint force significantly influenced the directions toward which endpoint stiffness orientation could be rotated ($P < 0.001$). Figure 6 shows the average effect of force direction on the ability to modulate endpoint stiffness orientation for all subjects. The thick solid line indicates the total range of modulation, the thin solid line shows the portion of this range due to counter clockwise rotations relative to the N task, and the dashed line indicates the portion of the range due to clockwise rotations relative to the N task. Although the total modulation range remained nearly constant with force direction, force direction significantly affected how the subjects were able to generate this range. Substantial clockwise rotations relative to the N task could not be generated when the voluntarily generated endpoint forces required only elbow torques. Similarly, substantial counter clockwise rotations could not be generated when the endpoint forces required only shoulder torques. Endpoint stiffness could be rotated both to the left and to the right when the endpoint forces were generated by both shoulder and elbow torques.

RELATIVE RANGE OF VOLUNTARY STIFFNESS MODULATION AND OBLIGATORY FORCE-RELATED MODULATION. The range of stiffness orientations that could be obtained with changes in voluntary effort was small relative those resulting from changes in endpoint force direction. Figure 7 shows the cross-subject averages of static endpoint stiffness orientation for the N tasks for each of the three required endpoint force directions (thick lines corresponding to E: elbow torque only, S: shoulder torque only, and ES: elbow and shoulder torques) as well as the average ranges over which the stiffness orientation could be modulated by visually guided voluntary effort for these three endpoint force directions (shaded arcs). The range of endpoint stiffness orientations observed during N tasks was 37.0°. This was approximately twice the 19.8° average orientation range that could be achieved with changes in voluntary effort while subjects were exerting forces against the manipulator. The range of orientations that could be achieved when there was no

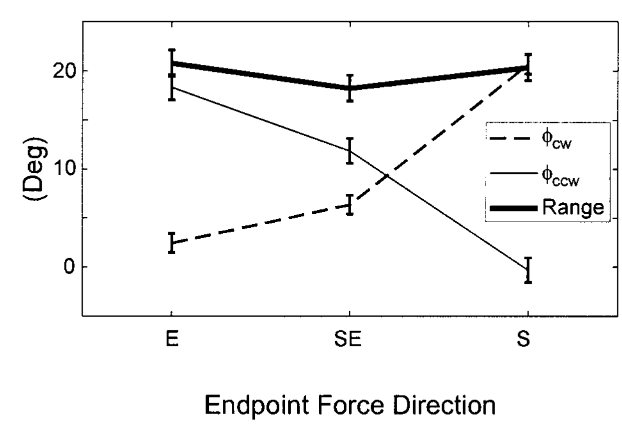

FIG. 6. Effects of force direction. The average effect of force direction on the ability to modulate endpoint stiffness orientation for all subjects is shown. The thick solid line indicates the total range, the thin solid line shows the range portion due to counter clockwise rotations relative to the N task, and the dashed line indicates the portion due to clockwise rotations relative to the N task. Error bars indicate ±SE as estimated from a repeated-measures ANOVA.

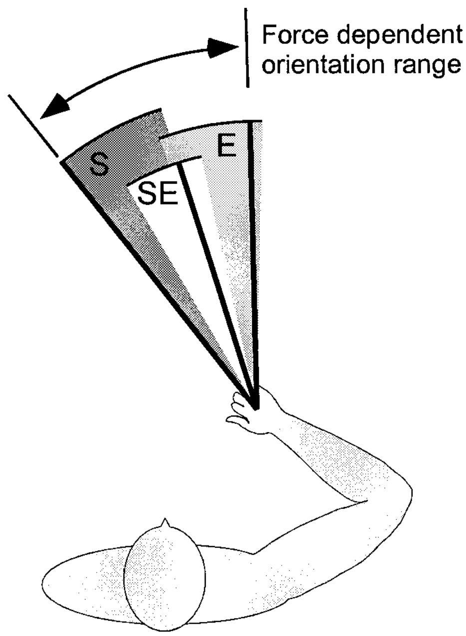

FIG. 7. Relative effects of voluntary effort and endpoint load. The average naturally occurring static endpoint stiffness orientation (thick solid lines) and the range (arcs) over which this orientation could be voluntarily modulated for all subjects is shown. Force directions are indicated by the letters in each of these arcs: (S) represents forces that required only shoulder torques, (E) is for the forces that required only elbow torques, and (SE) is for the forces that required both elbow and shoulder torques.

net force present at the hand was between these two values (29.8°, see Fig. 5). These results indicate that the available stiffness orientation range depended significantly on the voluntary force subjects were required to exert.

Joint-stiffness modulation

To examine the physiological mechanisms underlying the observed modulation of endpoint stiffness orientation, joint-stiffness parameters were calculated using *Eq. 7*. As in previous studies (Mussa-Ivaldi et al. 1985; Perreault et al. 2001; Tsuji et al. 1995), the joint-stiffness matrices were predominantly symmetric. The median ratio of the anti-symmetric component area to that of the symmetric component was 2% across all trials for all subjects. Therefore only the symmetric component was used to simplify further analyses at the joint level. Regression was used to determine if there was synergistic activation of the single- and cross-joint muscles by fitting a linear model between the stiffness contributions of the single joint muscles crossing the elbow and shoulder joints (K_e and K_s in *Eq. 8*) and the cross-joint stiffness (K_x) for all trials during which subjects attempted to modulate stiffness orientation. The average R^2 of this model across all subjects was 0.37, indicating a modest coupling between the actions of the single- and cross-joint muscles. In contrast, the single-joint muscles crossing the elbow and shoulder joints acted nearly independently (mean $r^2 = 0.12$). In most trials, the magnitude of the cross-joint stiffness was less than that contributed by the single-joint muscles. Single-joint muscle-stiffness magnitudes at the elbow and shoulder were greater than that of the cross-joint stiffness in 97 and 84% of the trials, respectively, suggesting that single-joint muscles were the dominant contributors to endpoint stiffness during most trials.

DISCUSSION

This work investigated the degree to which humans can modulate static endpoint stiffness orientation while exerting voluntary forces against a rigid object. Real-time feedback of endpoint stiffness orientation was used to assist in this task. We found that individuals can voluntarily change stiffness orientation but that the magnitude of these changes is small relative to those that arise from obligatory changes due to endpoint force generation, the range of available voluntary stiffness orientations decreases with increasing endpoint forces, and the direction of the force at the endpoint strongly affects how endpoint stiffness orientation can be changed. These findings suggest that separate neural control of endpoint force and endpoint stiffness orientation is unlikely during postural tasks.

Methodology

Real-time feedback was used to provide subjects with a constant visual representation of their static endpoint stiffness. This was accomplished by implementing a recursive, parametric, system identification algorithm to estimate the stiffness dynamics relating endpoint forces and displacements during stochastic perturbations of the hand. This approach differs from the robust, off-line, nonparametric methods typically used in our lab (Perreault et al. 1999, 2001). However, we found that the steady-state differences between the static stiffness characteristics estimated by both algorithms were small. Ellipse orientation, which was of primary importance in this study, differed by only 0.91 ± 5.85°.

The major limitation of the visual feedback for the goals of this study was the delay between the occurrence of changes in endpoint stiffness and the time required for those changes to be accurately displayed to the subject. Because of this inherent limitation of any real-time stiffness estimate, we were not able to track rapid changes in endpoint stiffness but only those that could be maintained for a period of time. Within this constraint, though, it is not likely that the slow convergence of this algorithm reduced subjects' ability to modify endpoint stiffness orientation. Although the time to convergence was approximately 15 s (see Fig. 3), subjects began to see changes in stiffness orientation soon after initiating their efforts and therefore had rapid feedback regarding whether or not their attempts to modulate stiffness orientation were successful. Only knowledge regarding the *degree* of this success was delayed.

Effects of force magnitude

Subjects were able to change stiffness orientation for all tested endpoint forces. The average orientation range that could be achieved when no forces were applied to the hand was 29.8°. This decreased to 21.3° when generating endpoint forces at 10% MVC and to 18.3° when generating 20% MVC forces. Gomi and Osu (1998) also investigated the ability to modulate endpoint stiffness orientation when no net force was present at the hand. Their study provided subjects with electromyographic feedback of a subset of the muscles responsible for regulating arm stiffness. Their subjects were given instructions on how to change the relative cocontraction of specific muscle groups, and the corresponding effects on endpoint stiffness were measured. Using this protocol, they also concluded that endpoint stiffness orientation could be modulated voluntarily.

Although they did not report the range of stiffness orientations that could be achieved, this appears to be between 25 and 30° for the arm posture most similar to that used in this study (Gomi and Osu 1998) (Figs. 3 and 5, PC posture). This is only slightly lower than the similar conditions measured in this study. The differences could simply be due to inter-subject variations or to the fact that we provided direct feedback of endpoint stiffness orientation not just muscle activity.

Effects of force direction

The direction of the endpoint force had a significant effect on the directions toward which endpoint stiffness could be rotated relative to the direction obtained when subjects simply matched the target force without regard to stiffness. Large clockwise rotations could not be generated when the endpoint forces required only elbow torques, and large counterclockwise rotations could not be generated when the endpoint forces required only shoulder torques. Increased elbow stiffness tends to rotate endpoint stiffness clockwise, while increased shoulder stiffness results in counter clockwise rotations (Gomi and Osu 1998). These effects are seen in Fig. 7, where the average ellipse orientation for forces requiring only elbow torques is rotated clockwise 37° relative to that for the forces requiring only shoulder torques. These results indicate that the voluntary rotation of endpoint stiffness is severely constrained by the simultaneous need to produce endpoint forces in a particular direction and implies a limitation in the flexibility of voluntary endpoint stiffness control.

Mechanisms underlying stiffness regulation

A wide range of endpoint stiffness orientations could be achieved if single- and cross-joint arm muscles could be activated independently (Gomi and Osu 1998; Hogan 1985), but this study has shown that the range of stiffness orientations that can be maintained during postural tasks is constrained severely. These results suggest a limitation on the flexibility of voluntary muscle activation during postural tasks. The mechanisms underlying this behavior were investigated by examining the contributions of single- and cross-joint muscles to the net arm stiffness. We found that the single-joint muscles crossing the shoulder and elbow joints could be activated independently but that the actions of the muscles spanning both of these joints were constrained by single-joint muscle activity. Approximately 40% of the cross-joint-stiffness variance was linearly related to the single-joint stiffnesses. Furthermore, the cross-joint stiffness was nearly always less than that contributed by the single-joint muscles.

The co-variation of cross-joint stiffness with changes in the stiffness of single-joint muscles suggests a neural constraint on the flexibility of voluntary muscle activation during postural tasks. Part of this limitation may arise from the inability to maximally cocontract muscle antagonists as reported previously (Kearney and Hunter 1990; Tyler and Hutton 1986). Milner et al. (1995) demonstrated that muscle inhibition during cocontraction was task dependent and could be reduced when subjects performed tasks that required increased joint stiffness. Hence it is possible that a greater range of endpoint stiffness orientations could be achieved in postural tasks different from those used in this study. Our results suggest though that if a greater modulation of endpoint stiffness orientations could be achieved, these modulations would involve subconscious rather than voluntary mechanisms. Recent results by Burdet et al. (2001) demonstrate that a subconscious, task-dependent modulation of stiffness orientation may occur during movement in unstable environments. Similar multi-joint studies have yet to be performed during postural tasks.

It is likely that voluntary control of endpoint stiffness orientation varies with changes in arm posture. The present study examined the voluntary control of stiffness orientation at a single arm posture as close to each subject's torso as was possible using the available apparatus. A hand position close to the torso was chosen to maximize the opportunity for modulating endpoint stiffness orientation. Previous simulation studies have shown that, for a fixed range of joint stiffnesses, a greater range of endpoint stiffness orientations can be obtained as the hand location is moved toward the torso. Hence, for the sagittal plane examined in this study, less voluntary control of endpoint stiffness orientation would be expected at more distal hand locations. In the absence of significant cocontraction, voluntarily generated endpoint forces have a greater effect on endpoint stiffness orientation at medial hand postures relative to that at more lateral hand postures. Therefore it is possible that greater voluntary control over stiffness orientation is also possible at more medial locations than that used in this study. Even though the range of endpoint stiffness orientations that can be achieved with changes in voluntary control is almost certain to vary with arm posture, the effects of voluntary changes in stiffness orientation relative to those resulting from changes in applied endpoint forces are less clear. Recent results showed that in the absence of significant cocontraction, joint stiffness-joint torque relationships are nearly posture independent (Perreault et al. 2001). If the ability to cocontract antagonistic muscle groups is also nearly posture-independent, the effects of voluntary efforts to modulate stiffness orientation are likely to be significantly less than the obligatory orientation changes resulting from exerting forces on the environment at all locations in the workspace. Tyler and Hutton (1986) reported invariant levels of elbow flexor cocontraction with changes in elbow angle, but some posture-dependent changes in elbow extensor cocontraction. Hence, further study is required to determine the extent of posture-dependent muscle activation constraints for the muscles regulating endpoint stiffness of the human arm.

Implications for the control of endpoint mechanics

The inertial, viscous and elastic properties of the arm all influence the mechanical interface humans use to interact with their environment (Hogan 1985; Lacquaniti 1993), and it is plausible that any of these properties are modulated by neural mechanisms during postural tasks. Endpoint inertia dominates the response to high-frequency perturbations of arm posture and the initial response to transient perturbations (Bennett et al. 1992). The orientation along which inertia provides the greatest resistance to these perturbations is dependent on arm orientation (see Hogan 1985 for a discussion). Hence choice of posture is likely to be an important control variable for manipulating endpoint stiffness dynamics during functional tasks but was not a factor in our study because the arm configuration was fixed.

As with inertia, endpoint viscosity contributes to the stiffness dynamics. Specifically, it describes how the arm dissipates energy imparted by external perturbations. Without viscosity, a system containing only elastic and inertial components would oscillate without decay when perturbed. During unloaded posture maintenance, endpoint stiffness and endpoint viscosity are co-oriented (Dolan et al. 1993; Tsuji et al. 1995), but this relationship does not necessarily hold when significant forces are generated at the hand (Perreault 2000), indicating that endpoint stiffness and endpoint viscosity orientation may be controlled independently. Lacquaniti (1993) provided evidence for this possibility by demonstrating a *subconscious*, transient modulation of endpoint viscosity orientation during the preparation for catching, although endpoint elasticity orientation remained invariant. The *voluntary* control of viscous properties remains to be studied, although preliminary studies indicated that the recursive algorithm used in this work was not able to provide robust estimates of endpoint viscosity. Therefore methods different from those employed in this study will need to be developed.

This study focused on the static or elastic stiffness properties of the arm, which are most relevant to the maintenance of posture. Specifically, we examined the degree to which changes in endpoint stiffness orientation could be maintained as individuals exert voluntary forces on the environment. Recent work (Burdet et al. 2001) suggests that large changes in stiffness orientation may be generated transiently, but our results clearly demonstrate that such changes cannot be maintained voluntarily. We found that although static endpoint stiffness orientation can be modulated voluntarily, the degree of modulation is small and constrained by voluntary force exertion. Previous studies and our results (see Fig. 4) indicate that increases in muscle activation dramatically increase static endpoint stiffness (Gomi and Osu 1998; McIntyre et al. 1996; Mussa-Ivaldi et al. 1985; Perreault et al. 2001). Because these changes are large compared with the changes in orientation that can be achieved, it is likely that voluntary control of static stiffness properties is dominated by changes in overall stiffness size rather than changes in stiffness orientation. In contrast, it appears unlikely that static endpoint stiffness orientation is actively controlled by voluntary neural mechanisms during sustained postural tasks.

The authors thank Dr. C. J. Heckman for comments on the manuscript.

This work was supported by the Department of Veteran Affairs Rehabilitation Research and Development Service, the National Institutes of Health, and the Cleveland Functional Electrical Stimulation Institute.

REFERENCES

ACOSTA AM, KIRSCH RF, AND PERREAULT EJ. A robotic manipulator for the characterization of two-dimensional dynamic stiffness using stochastic displacement perturbations. *J Neurosci Methods* 102: 177–186, 2000.

BENNETT DJ, HOLLERBACH JM, XU Y, AND HUNTER IW. Time-varying stiffness of the human elbow joint during cyclic voluntary movement. *Exp Brain Res* 88: 433–442, 1992.

BIZZI E AND ABEND W. Posture control and trajectory formation in single- and multi-joint movements. In: *Advances in Neurology: Motor Control Mechanisms in Health and Disease*, edited by Desmedt J. New York: Raven, 1983, p. 31–45.

BURDET E, OSU R, FRANKLIN DW, MILNER TE, AND KAWATO M. The central nervous system stabilizes unstable dynamics by learning optimal impedance. *Nature* 414: 446–449, 2001.

COLGATE JE AND HOGAN N. Robust control of dynamically interacting systems. *Int J Control* 48: 65–88, 1988.

DOLAN JM, FRIEDMAN MB, AND NAGURKA ML. Dynamic and loaded impedance components in the maintenance of human arm posture. *IEEE Trans Syst Man Cybern* 23: 698–709, 1993.

FELDMAN AG. Functional tuning of nervous system with control of movement or maintenance of a steady posture. III. Mechanographic analysis of the execution by man of the simplest motor tasks. *Biofizika* 11: 667–675, 1966.

GOLUB GH AND VAN LOAN CF. *Matrix Computations*. Baltimore, MD: Johns Hopkins University Press, 1996.

GOMI H AND KAWATO M. Human arm stiffness and equilibrium-point trajectory during multi-joint movement. *Biol Cybern* 76: 163–171, 1997.

GOMI H AND KONNO T. Real time estimation of time-varying human multijoint arm viscoelasticity during movements. *Proc Int Conf IEEE/EMBS* 20: 2341–2342, 1998.

GOMI H AND OSU R. Task-dependent viscoelasticity of human multijoint arm and its spatial characteristics for interaction with environments. *J Neurosci* 18: 8965–8978, 1998.

HOGAN N. The mechanics of multi-joint posture and movement control. *Biol Cybern* 52: 315–331, 1985.

KEARNEY RE AND HUNTER IW. System identification of human joint dynamics. *CRC Crit Rev Biomed Eng* 18: 55–87, 1990.

LACQUANITI F, CARROZZO M, AND BORGHESE NA. Time-varying mechanical behavior of multijointed arm in man. *J Neurophysiol* 69: 1443–1463, 1993.

LJUNG L. *System Identification Theory for the User*. Englewood Cliffs, NJ: Prentice-Hall, 1987.

MANN KA, WERNER FW, AND PALMER AK. Frequency spectrum analysis of wrist motion for activities of daily living. *J Orthop Res* 7: 304–306, 1989.

MCINTYRE J, MUSSA-IVALDI FA, AND BIZZI E. The control of stable arm postures in the multi-joint arm. *Exp Brain Res* 110: 248–264, 1996.

MILNER TE, CLOUTIER C, LEGER AB, AND FRANKLIN DW. Inability to activate muscles maximally during cocontraction and the effect on joint stiffness. *Exp Brain Res* 107: 293–305, 1995.

MONTGOMERY DC. *Design and Analysis of Experiments*. New York: Wiley, 1991.

MUSSA-IVALDI FA, HOGAN N, AND BIZZI E. Neural, mechanical, and geometric factors subserving arm posture in humans. *J Neurosci* 5: 2732–2743, 1985.

PERREAULT EJ. *Control of Arm Stiffness During Force Regulation Tasks: Able-Bodied Strategies and Changes Following Cervical Spinal Cord Injury* (PhD thesis). Cleveland, OH: Case Western Reserve University, 2000.

PERREAULT EJ, KIRSCH RF, AND ACOSTA AM. Multiple-input, multiple-output system identification for the characterization of limb stiffness dynamics. *Biol Cybern* 80: 327–337, 1999.

PERREAULT EJ, KIRSCH RF, AND CRAGO PE. Voluntary control of static endpoint stiffness. *Soc Neurosci Abstr* 26: 171, 2000.

PERREAULT EJ, KIRSCH RF, AND CRAGO PE. Effects of voluntary force generation on the elastic components of endpoint stiffness. *Exp Brain Res* 141: 312–323, 2001.

STROEVE S. Impedance characteristics of a neuromusculoskeletal model of the human arm. I. Posture control. *Biol Cybern* 81: 475–494, 1999.

TSUJI T, MORASSO PG, GOTO K, AND ITO K. Hand impedance characteristics during maintained posture. *Biol Cybern* 72: 475–485, 1995.

TYLER AE AND HUTTON RS. Was Sherrington right about co-contractions? *Brain Res* 370: 171–175, 1986.